

ELECTROCHEMICAL PERFORMANCE OF THE POROUS NICKEL ANODE IN THE MOLTEN CARBONATE FUEL CELL

Göran Lindbergh and Mari Sparr

Department of Chemical Engineering and Technology, Applied Electrochemistry,
Royal Institute of Technology, SE-100 44 Stockholm, Sweden

ABSTRACT

In this study, stationary polarisation curves were obtained for a porous nickel electrode under varying temperatures and anode gas compositions. The exchange current densities were determined from the slopes of the polarisation curves at low overpotentials, *i.e.* the assumption was made that the porous electrode is under kinetic control. The outlet gas compositions were measured by analysis in a gas chromatograph. The gases were found to be far from equilibrium. However, almost the same reaction orders were found independently of the assumptions of gas compositions but they were rather high and therefore difficult to be explained by the generally assumed mechanisms.

INTRODUCTION

In a fuel cell, chemical energy in a fuel is continuously and directly converted to electrical energy by means of electrochemical reactions taking place on the anode and the cathode. Several fuel cell types are under development, differing in operating temperature and materials used for electrolyte and electrodes. The molten carbonate fuel cell (MCFC) operates at a high temperature (600-700°C), which gives it the potential to reach high overall electrical efficiency (50-60%) in an integrated system. It is generally operated using natural gas as its fuel, although it can also operate with high concentrations of carbon monoxide and carbon dioxide in the fuel, making it very suitable for use with biogas or gasified biomass feeds.

The MCFC is step by step coming closer to commercialisation, with several large units in the MW scale demonstrated during the last years. The state-of-the-art technology consists of an in-situ oxidised porous nickel oxide cathode, a porous nickel anode and a lithium-potassium or lithium-sodium carbonate melt as electrolyte. Both the cathode and the anode are so called gas diffusion electrodes, made up of larger pores for gas transport, smaller pores filled by molten alkali carbonate and a solid electron conducting electrode matrix. The reactants are transported into the electrode in the gaseous phase, dissolved in the melt and reacted at the electrode surface.

Operation of MCFC with biogas or biomass will result in much lower concentrations of hydrogen gas in the fuel. Therefore it is of interest to investigate the performance of the anode under such conditions. The overvoltage losses at the anode are considered to be relatively small, which partly is due to the relatively low current densities that present MCFC systems are operating at. A significant increase in this, which is desirable in order to improve the power density, would result in increase of losses at the anode. Operating with lower concentration of hydrogen is also expected to increase the losses at the anode.

A general procedure when elucidating the mechanism of the anode reaction is to determine the reaction orders for the components (H_2 , CO_2 and H_2O) that are involved in the overall electrochemical reaction.



Several studies have been made to find out the reaction mechanism at the anode, Table 1. Most experiments were conducted on flag electrodes, which are quite different from porous electrodes, regarding electrode material and mass transfer conditions. Though a lot of research has been done the reaction mechanism is still not well known.

A problem when evaluating the reaction orders is to know the gas composition inside the cell since other reactions can take place at the anode. Carbon monoxide can be oxidised electrochemically.



Another possible reaction is the shift reaction, which is the electrically neutral sum of reaction [1] and [2].



According to Borucka and Appleby (19) the reaction rate for direct CO oxidation is extremely slow at 99.99% pure gold. They claimed that the most likely way for the CO to be utilised is through the shift reaction that has been reported to be established rapidly (20).

In this study, stationary polarisation curves were obtained for the porous electrode under varying anode gas compositions at 600, 650 and 700°C. The slopes of the polarisation curves were studied at low overpotentials and high flow rates and the exchange current densities were determined from these curves. Since it is not possible to investigate the hydrogen oxidation without interference by other reactions it is necessary to control the gas composition. The gas flow as well as the inert gas were varied to examine the effect of mass transfer limitations in the gas phase.

The objectives of the study are to get a better understanding of the factors that influence cell performance at the anode side, to determine the kinetic parameters of the hydrogen oxidation reaction and to obtain information about the reaction mechanism, even at low concentrations of hydrogen. The results can be used in cell and stack models for system simulations as well as for stack design.

EXPERIMENTAL

Experimental data were obtained from a 3 cm² laboratory cell unit provided by ECN, The Netherlands. The cell consisted of a porous nickel anode alloyed with 10%Cr, a porous nickel cathode, that was oxidised *in situ*, and a LiAlO₂ matrix, supporting a 62% Li₂CO₃/ 38% K₂CO₃ electrolyte. The reference electrodes were gold wires submerged into the melt and in equilibrium with a 33/67% O₂/CO₂ gas mixture. The reference electrodes were connected to the cell via small capillaries in the cell house. All the experiments were carried out with standard cathode gas, *i.e.*, 15/30% O₂/CO₂ in N₂. Different anode gases were used for the experiments. In order to reduce the effect of mass transfer limitations in the gaseous phase and conversion, the gas flow rate was kept high (225 ml/min). These gases were fed into the cell after saturating them with water vapour. The anode gases were humidified at 60°C and the cathode gases were humidified at 30°C. The cell temperature was varied between 600, 650 and 700°C. At each temperature, polarisation curves were obtained. In order to get cell conditions more like a real cell, where it is usually assumed that the gas has reached equilibrium, some catalyst was placed in the gas channel inlet for cell no. 1 and cell no. 3. A nickel wire netting was inserted in the gas channel for cell no.1 and a commercial shift reactor was used in the same way for cell no.3.

Polarisation curves for different gas compositions were all obtained at optimal electrolyte filling by a Solartron 1286 Electrochemical Interface. For evaluation of the ohmic potential drop, the current interrupt method was used. In these measurements the overvoltage was recorded 20 µs after interruption of the current.

THEORY

The exchange current densities for different fuel gases were determined on the basis of the polarisation curves. When analysing experimental data from porous electrodes it is important to take into account the current distribution along the depth of the electrode. According to

Lagergren and Simonsson (22) this could be done by the expression for the total polarisation resistance.

$$\frac{d\eta}{di} = \frac{L}{\kappa_1 + \kappa_2} + \frac{L}{\sqrt{a}} \cdot \frac{1}{\kappa_1 + \kappa_2} \cdot \left[\frac{2}{\sinh \sqrt{a}} + \left(\frac{\kappa_1}{\kappa_2} + \frac{\kappa_2}{\kappa_1} \right) \cdot \coth \sqrt{a} \right] \quad [1]$$

$$a = \frac{L^2 F S i_0 n}{RT} \cdot \left(\frac{1}{\kappa_2} + \frac{1}{\kappa_1} \right) \quad [2]$$

The equation has asymptotic equations that may be found for the two limiting cases, when a approaches zero and infinity. With the assumption that a is large and that the electrodes effective conductivity κ_1 is much higher than the pore electrolyte conductivity (κ_2), one obtains

$$\frac{d\eta}{di} = \sqrt{\frac{RT}{n F S i_0 \kappa_2}} \quad [3]$$

which is valid also for the anode under following conditions:

- The external agglomerate surface area S , was estimated to be $2.7 \cdot 10^5 \text{ m}^{-1}$, by assuming that the agglomerate are spherical and with a radius of $4 \text{ }\mu\text{m}$.
- Only the external surface of the agglomerates is accessible for the reaction.
- The porosity of the electrode was 64% and the pore electrolyte conductivity was assumed to be 5 S/m at 650°C .

This means that at low overpotentials, where mass transfer limitations are assumed to be small, there is a proportional relationship between the current density and the overpotential. The exchange current density is a function of the partial pressure of the reactants according to

$$i_0 = i_0^0 \cdot P_{H_2}^a \cdot P_{CO_2}^b \cdot P_{H_2O}^c \quad [4]$$

where a , b , and c are the partial pressure dependency for H_2 , CO_2 and H_2O , respectively, and i_0^0 is the standard exchange current density.

RESULTS AND DISCUSSION

The reaction orders were calculated by solving the over-determined system [4]. The same reaction orders were found to be valid for the complete temperature range. In case I, the water content in all gases was close to that in the inlet gas (always 19.9%) which made the reaction order of water more uncertain. The results are shown in Table 2. These reaction orders are rather high and therefore difficult to be explained by the generally assumed mechanisms.

A commercial catalyst for the water-shift reaction was placed in the gas channel for cell no.3 to facilitate the reaction. Tables 3 and 4 shows the reaction orders for cell number 2 and 3. They are similar to those obtained from cell number 1 though the cell performance was better for the last two cells (fig. 1). This figure also shows that the performance was the same for cell no.2 and

3 though the third cell had a commercial catalyst and no.2 did not have any catalyst. These two cells showed almost the same performance for all the gases except that the temperature dependence was larger for the third cell.

The obtained exchange current density, for standard gas at 650°C, is 70 A/m². The temperature dependence of the exchange current density is small with an activation energy of 40-65 kJ/mol. This value is in the same range as those reported by other authors [8,15].

Concluding this section, the obtained results could be used in cell and stack models for system simulations as well as for stack design. Further work is still necessary since our model gives a better description of the performance but still not the whole truth and not a perfect description of the cell performance under varying gas composition.

CONCLUSIONS

This study has gone some way towards understanding of the anode reaction in MCFC. It has highlighted a number of problem areas in existing theory and further research is still needed.

Almost the same reaction orders were found for cell no. 1-3 though the cell performance was better for the last two cells. However, they were rather high and therefore difficult to explain by the generally assumed mechanisms. The obtained exchange current density, for standard gas at 650°C is 70 A/m² and the activation energy is 40-65 kJ/mol.

ACKNOWLEDGMENTS

This work was financially supported by the Swedish National Energy Administration and the International Joint Research grant, NEDO (Japan). The laboratory cell unit and the cell components are purchased from ECN in the Netherlands.

List of symbols

F	Faraday's number [As/mol]
i	current density [A/m ²]
i ₀	exchange current density [A/m ²]
i ₀ ⁰	standard exchange current density [A/m ²]
L	electrode thickness [m]
n	number of electrons
R	gas constant [J/mol K]
S	specific surface area [m ⁻¹]
T	temperature [K]
Greek letters	
ε	effectiveness factor
κ ₁	conductivity in electrode phase [S/m]
κ ₂	conductivity in electrolyte phase [S/m]
η	overpotential [V]

REFERENCES

1. P. G. P. Ang and A.F. Sammells, *J. Electrochem. Soc.*, **127**, 1287, (1980)
2. W. M. Vogel, L. J. Bregoli and S. W. Smith, *J. Electrochem. Soc.*, **127**, 833, (1980)
3. J. Jewulski and L. Suski, *J. Appl. Electrochem*, **14**, 135, (1984)
4. S. H. Lu and J. R. Selman, *J. Electrochem. Soc.*, **131**, 2827, (1984)
5. S. H. Lu and J. R. Selman, *J. Electrochem. Soc.*, **136**, 1063, (1989)
6. S. H. Lu and J. R. Selman, *J. Electrochem. Soc.*, **136**, 1068, (1989)
7. C. Y. Yuh and J. R. Selman, *J. Electrochem. Soc.*, **131**, 2062, (1984)
8. C. Y. Yuh and J. R. Selman, *J. Electrochem. Soc.*, **138**, 3642, (1991)
9. C. Y. Yuh and J. R. Selman, *J. Electrochem. Soc.*, **138**, 3649, (1991)
10. C. Y. Yuh and J. R. Selman, *J. Electrochem. Soc.*, **139**, 1373, (1992)
11. L. K. Bieniasz and L. Suski, *J. Electroanal. Chem.*, **249**, 155, (1988)
12. T. Nishina, M. Takahashi and I. Uchida, *J. Electrochem. Soc.*, **137**, 1112, (1990)
13. R. Weewer, R. C. Makkus, K. Hemmes and J. H. de Wit, *J. Electrochem. Soc.*, **137**, 3156, (1990)
14. R. Weewer, PhD thesis, The Netherlands, (1991)
15. R. Weewer, K. Hemmes and J. H. de Wit, *J. Electrochem. Soc.*, **142**, 389, (1995)
16. G. Wilemski, *J. Electrochem. Soc.*, **130**, 117, (1983)
17. L. Bieniasz and L. Suski, *Polish J. Chem.*, **71**, 407, (1997)
18. P. S. Christensen and H. Livbjerg, *Chemical Engineering Science*, **47**, 2933 (1992)
19. A. J. Appleby and A. Borucka, *J. Chem. Soc., Faraday Trans. 1*, **73**, 1420 (1977)
20. S.H. Clarke et al., *Catalysis Today*, **38**, 411, (1997)
21. C. Lagergren, A. Lundblad and B. Bergman, *J. Electrochem. Soc.*, **141**, 2959, (1994)
22. C. Lagergren and D. Simonsson, *J. Electrochem. Soc.*, **144**, 3813, (1997)
23. Y. Magikura and J.R. Selman, *J. Electrochem. Soc.*, **143**, 2442, (1996)

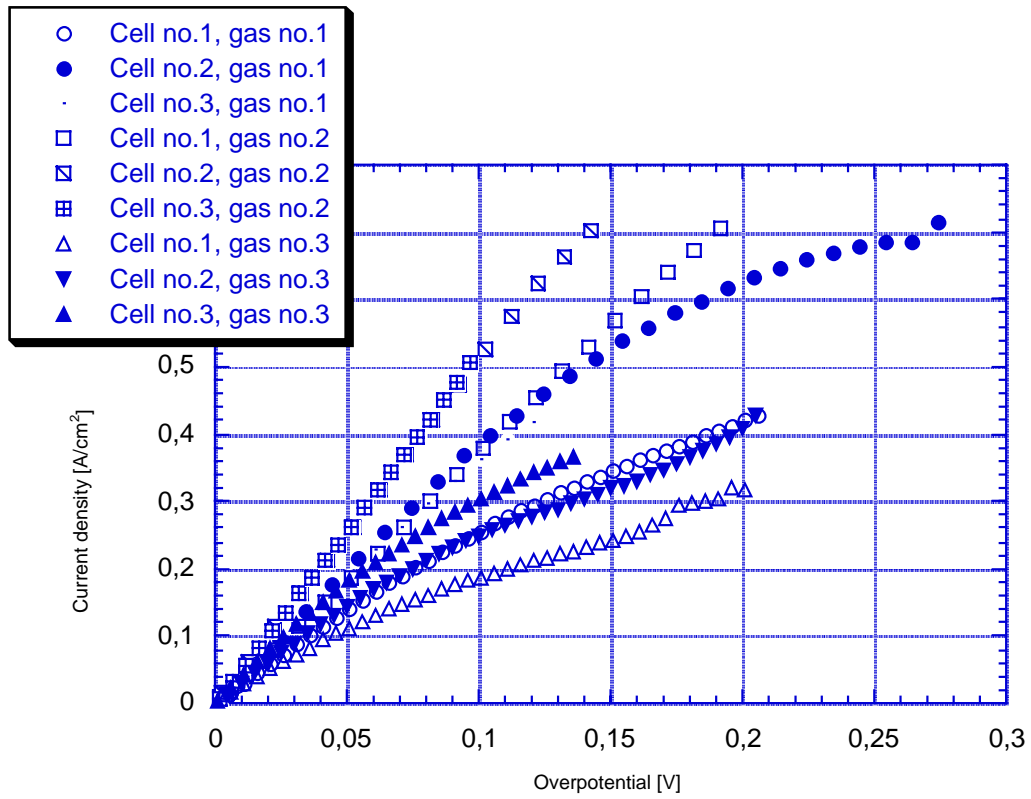


Fig. 1: Polarisation curves for the porous nickel anode at 650°C for different gas compositions.
 Gas no.1: 16% H₂, 32% CO₂, 20% H₂O and N₂, gas no. 2: 64% H₂, 16% CO₂ and 20% H₂O,
 gas no. 3: 6% H₂, 67% CO₂, 7% CO and 20% H₂O.

Table 1: Published work on the anode kinetics and mechanism. Experimental conditions. (EIM=impedance measurement, CA=chronoamperometry, CC=chronocoulometry, CV=cyclic voltammetry)

References	Years	Techniques	Electrodes
Ang & Sammells (1)	1980	polarization, CA	Ni, Co wire
Vogel (2)	1980	polarization	Ni, Au, Pt flag Ni membrane-porous
Jewulski & Suski (3)	1984	calculations	
Lu & Selman (4)	1984	polarization, CA	Ni, Cu cylinder
(5-6)	1989	CV, calculations	Cu wire
Yu & Selman (7)	1984	calculations	Ni porous Ni porous
(8)	1991	polarization	
(9)	1991	IM	
(10)	1996	calculations	
Bieniasz & Suski (11)	1988	Calculations	Au (Ni, Co, Cu)
Nishina et al. (12)	1990	IM, CV, CC	Ni, Co, Cu, Au, Ag, Pt, Pd, Ir flag
Weewer et al. (13)	1990	IM	Ni
Weewer (14)	1991	polarization, IM,	Ni, Au, Cu flag, Ni porous
Weewer et al. (15)	1995	CV, CA	
Wilemski (16)	1983	Calculations	
Suski (17)	1997	Review article	
Christensen & Livbjerg (18)	1992	calculations	Ni

Table 2: Partial pressure dependency for H₂, CO₂ and H₂O. Cell no. 1

	a	b	c
Measured	0.50 +/- 0.15	0.50 +/- 0.22	1.25 +/- 2.24
Equilibrium	0.75 +/- 0.14	0.62 +/- 0.13	0.92 +/- 0.32

Table 3: Partial pressure dependency for H₂, CO₂ and H₂O. Cell no. 2

	a	b	c	i ₀ [A/m ²]	E _a [kJ/mol]
Equilibrium	0.50 +/- 0.21	0.40 +/- 0.18	0.88 +/- 0.94	71	-42 +/- 13

Table 4: Partial pressure dependency for H₂, CO₂ and H₂O. Cell no. 3

	a	b	c	i ₀ [A/m ²]	E _a [kJ/mol]
Equilibrium	0.60 +/- 0.17	0.64 +/- 0.17	0.55 +/- 0.23	70	-65 +/- 12

i₀ is given at standard conditions *i.e.* 80% H₂ & 20% CO₂ humidified at 60°C. Operating temperature is 650°C.